Mechatronics and Intelligent Transportation Systems
https://www.acadlore.com/journals/MITS

Optimising Dual Pantograph-Catenary System Performance in Curved Sections for Enhanced High-Speed Railway Operations

Zhao Xu[1*], Jiaming Xiong[2], Wen Wang[1,3], Guobin Lin[1], Zhigang Liu[3]

[1] National Maglev Transportation Engineering R&D Center, Tongji University, 201804 Shanghai, China
[2] Zhongnan Engineering Corporation Limited. Powerchina, 410014 Changsha, China
[3] Department of Institute of Rail Transit, Tongji University, 201804 Shanghai, China

* Correspondence: Zhao Xu (xuzhao94@foxmail.com)

Received: 05-10-2024 **Revised:** 06-15-2024 **Accepted:** 07-10-2024

Citation: Z. Xu, J. M. Xiong, W. Wang, G. B. Lin, and Z. G. Liu, "Optimising dual pantograph-catenary system performance in curved sections for enhanced high-speed railway operations," *Mechatron. Intell Transp. Syst.*, vol. 3, no. 3, pp. 146–155, 2024. https://doi.org/10.56578/mits030301.

Abstract: The spatial configuration of the pantograph-catenary system (PCS) is significantly altered by the superelevation present in curved railway tracks, leading to deviations in the system's dynamic behaviour and imposing constraints on operational speeds. In this study, a detailed model of the PCS in curved sections has been developed to evaluate the dynamic performance of a dual PCS under these conditions. It was observed that the contact loss rate of the trailing pantograph increases markedly as train speed rises, with this effect being more pronounced in curved sections compared to straight tracks. This degradation in performance necessitates optimisation strategies to ensure operational efficiency at higher speeds. To address the issue, it is proposed that the static uplift force of the trailing pantograph be increased when trains traverse curved sections. Additionally, optimisation of the catenary system is recommended, involving both a reduction in the span length and an increase in the tension of the contact wire. By implementing these strategies, the dual PCS can sustain the necessary contact and satisfy dynamic performance criteria at speeds of up to 300 km/h in curved sections. These findings provide valuable insights for improving the reliability and safety of high-speed railway operations on complex track geometries.

Keywords: High-speed railway; Pantograph-catenary system (PCS); Curved sections; Dynamic performance; Finite Element Method (FEM); Optimization strategies

1 Introduction

Rail transit systems have emerged as an efficient solution for the rapid transportation of large populations. The key areas of development in China currently include urban rail transit, high-speed railways, and maglev systems [1]. Among these, high-speed rail has gained significant popularity, becoming a primary mode of transportation. High-speed trains are powered by electrical energy, which is supplied through the sliding contact between a pantograph mounted on the train's roof and the catenary system suspended above the tracks [2]. The dynamic interaction between the pantograph and the catenary is a critical factor influencing the current collection quality and, consequently, the operational reliability of the high-speed railway system. When trains navigate curved sections (depicted in Figure 1), they experience centrifugal forces, which must be counteracted to ensure stability. This is typically achieved through the use of superelevation, wherein the gravitational force of the train is employed to balance the centrifugal force. However, the tilting motion of the train in curved sections causes a lateral displacement of the pantograph on the train's roof, altering its operating position. This displacement changes the contact angle between the pantograph head and the contact wire, adversely affecting the dynamic performance of the PCS. The altered dynamics in curved sections are a critical factor limiting the operational speed of high-speed trains. Despite the importance of this issue, most existing studies on the dynamic performance of PCS have been conducted on straight track sections [3].

The FEM has been widely adopted as the dominant approach for modelling the PCS, with extensive use in recent research [3]. In the catenary system, various components are modelled using different element types: the contact wire, messenger wire, steady arm, and stitch wire are represented by beam elements, droppers are modelled as nonlinear springs, and clamps are treated as mass elements [4, 5]. To accurately represent the static displacement of the catenary system, it is necessary to determine the system's initial equilibrium state through static analysis [6].

The pantograph, on the other hand, is typically modelled as a lumped-mass system [7], and its interaction with the catenary is coupled via the penalty function method [8].

Figure 1. High-speed trains pass through curves

The dynamic performance of the PCS is typically evaluated using indicators such as contact force, contact loss rate, and the dynamic uplift of the contact wire [9]. Among these, contact force is regarded as a critical parameter, directly reflecting the dynamic performance of the system [7]. Several studies have identified key factors influencing PCS performance, including wave propagation in the contact wire [10], as well as irregularities in the wire's geometry [11, 12]. In addition, external disturbances, such as wind loads [13, 14] and vehicle-track interactions [15], have also been shown to impact the system's behaviour.

While significant research has been conducted on PCS performance in straight sections, studies focusing on curved sections remain limited. Existing research in this area primarily addresses the precise description of the catenary's geometric profile and the movement trajectory of the pantograph in curved sections. These studies have demonstrated considerable differences in the dynamic behaviour of the PCS between straight and curved tracks [16, 17].

Given the unique spatial geometry of the catenary system and the specific operational conditions of pantographs in curved sections, further investigation is warranted. Building upon previous work [17] that analysed the mathematical characteristics of curved catenaries and pantographs, the present study models the PCS in curved sections using design and line parameters from a high-speed railway in China. The dynamic performance of a dual PCS in curved sections is analysed, and optimisation strategies for both the pantograph and catenary are proposed to enhance operational speed in these challenging track geometries.

2 PCS Modeling

The stitched catenary comprises the messenger wire, contact wire, stitch wire, dropper, steady arm, and clamps, as illustrated in Figure 2. The Timoshenko beam theory is applied to model the contact wire, messenger wire, stitch wire, and steady arm. The droppers are modeled using nonlinear spring elements, while all clamps are represented as concentrated masses.

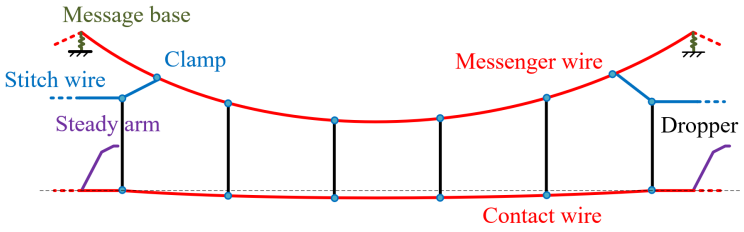

Figure 2. Schematic of stitched catenary

Based on the FEM, the motion equation of the catenary can be written as:

$$\mathbf{M}_{\mathrm{c}}\ddot{\mathbf{U}}_{\mathrm{c}} + \mathbf{C}_{\mathrm{c}}\dot{\mathbf{U}}_{\mathrm{c}} + \mathbf{K}_{\mathrm{c}}\mathbf{U}_{\mathrm{c}} = \mathbf{F}_{\mathrm{c}} \tag{1}$$

where $\ddot{\mathbf{U}}_{\mathrm{C}}$, $\dot{\mathbf{U}}_{\mathrm{C}}$ and $\mathbf{U}_{\mathrm{C}}$ are the acceleration, velocity, and displacement vectors of the catenary, respectively. $\mathbf{M}_{\mathrm{C}}$ is the mass matrix of catenary and $\mathbf{K}_{\mathrm{C}}$ is the stiffness matrix, $\mathbf{F}_{\mathrm{C}}$ is the external force vector of the catenary system. $\mathbf{C}_{\mathrm{C}}$ is the Rayleigh damp matrix of catenary. The specific modeling methods have been demonstrated in previous work [5].

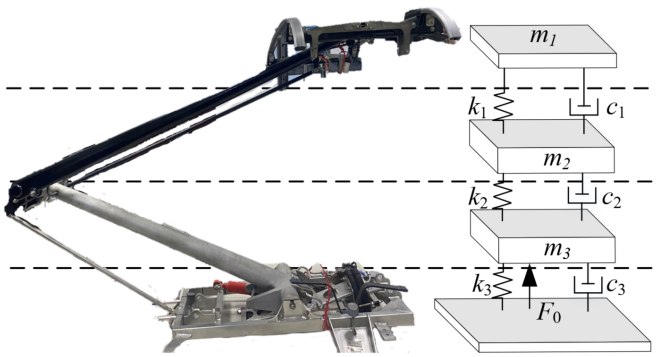

Figure 3. Lumped-mass model of pantograph

The pantograph is represented by lumped-mass system, as shown in Figure 3. m_1, m_2, m_3 are the equivalent masses of the pantograph. k_1, k_2, k_3 are the equivalent stiffnesses of the pantograph. c_1, c_2, c_3 are the equivalent damping of the pantograph. F_0 is the static uplift force of the pantograph. The penalty function has been adopted to couple the pantograph with the catenary. The expression of the penalty function method is:

$$f_c = \begin{cases} k_c \left(y_p - y_c\right) & y_p \geq y_c \\ 0 & y_p < y_c \end{cases} \tag{2}$$

where, f_c is the contact force between the contact wire and the pantograph head. y_c is the vertical uplift of contact wire, y_p is the vertical displacement of the pantograph head, k_c is the contact stiffness between catenary and pantograph.

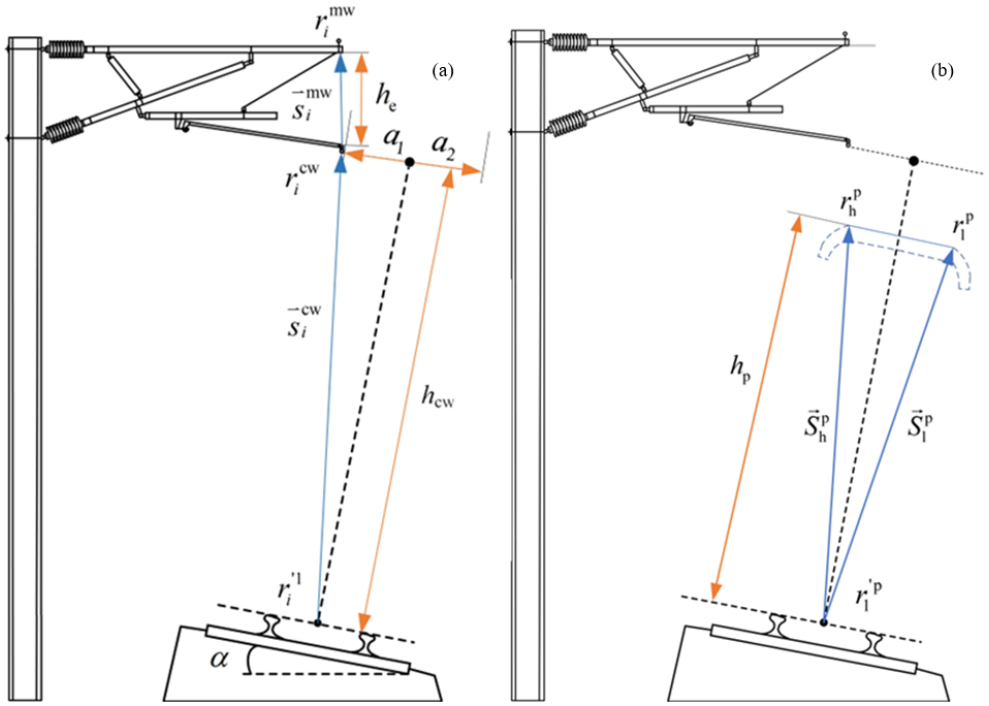

Figure 4. Diagram of curved characteristics: (a) Catenary model; (b) Pantograph model

The curved characteristics of the catenary system arise from its unique spatial geometric distribution and the operational state of the pantograph in curved sections, influenced by track surface inclination, as illustrated in Figure 4. In the catenary model, h_e is the encumbrance of catenary, h_{cw} is the contact wire height perpendicular to the track surface, a_1 and a_2 are the stagger values of adjacent steady points, $r_i'^1$ and $\vec{S}_i^{cw}$ are the coordinate vector and direction vector of the track center corresponding to the i-th steady point, r_i^{cw} and r_i^{mw} are the spatial coordinates of the i-th steady point and the messenger base, respectively, they can be represented as:

$$\begin{cases} r_i^{\mathrm{cw}} = r_i'^{1} + \vec{S}_i^{\mathrm{cw}} \\ r_i^{\mathrm{mw}} = r_i^{\mathrm{cw}} + \vec{S}_i^{\mathrm{mw}} \end{cases} \tag{3}$$

In the pantograph model, h_p is the height of the pantograph head relative to the track surface. $r_{\mathrm{h}}^{\mathrm{p}}$ and $r_{\mathrm{l}}^{\mathrm{p}}$ are the high point of the pantograph stripe on the outside of the track and the low point on the inside, respectively, $\vec{S}_{\mathrm{h}}^{\mathrm{p}}$ and $\vec{S}_{\mathrm{l}}^{\mathrm{p}}$ are the direction vector of those two points. $r_i'^{p}$ is the coordinate vector of the track center corresponding to the pantograph location. The spatial coordinates of the two endpoints of the pantograph stripe are:

$$\begin{cases} r_{\mathrm{h}}^{\mathrm{p}} = r_1'^{\mathrm{p}} + \vec{S}_{\mathrm{h}}^{\mathrm{p}} \\ r_{\mathrm{l}}^{\mathrm{p}} = r_1'^{\mathrm{p}} + \vec{S}_{\mathrm{l}}^{\mathrm{p}} \end{cases} \tag{4}$$

The accuracy of the model was validated in the author's previous work [17, 18], making it suitable for research on increasing the speed of the PCS in curved sections.

3 Research on Dynamic Performance of Dual Pantographs in Curved Sections

In this section, a dynamic coupling model of the PCS in curved sections is applied to study the dynamic performance under high-speed conditions. The model parameters are listed in Table 1.

Table 1. Parameters of pantograph-catenary model

Material Property of Catenary	
Contact wire	Tension: 25 kN; Young's modulus: 120 kN/mm^2; Mass per meter: 1.331 kg/m; Cross section; 150 mm^2
Messenger wire	Tension: 20 kN; Young's modulus: 120 kN/mm^2; Mass per meter: 1.106 kg/m; Cross section; 120 mm^2
Stitch wire	Tension: 3.5 kN; Young's modulus: 110 kN/mm^2; Mass per meter: 0.31 kg/m; Cross section; 35 mm^2
Dropper	Mass per meter: 0.089 kg/m; Tensile stiffness: 105 N/m
Clamps	Mass: 155 g (With CW); 140 g (With MW)
Messenger wire support	Fixed
Geometrical Property of Catenary	
Length of span: 50 m; Number of spans: 30; Stitch wire length: 18 m; Stagger value: 0.3 m; Interval of droppers: 8 m; Number of droppers: 6; Encumbrance:1.6 m; Steady arm stiffness: 1.25×10^7 N/m	
Lumped Mass Property of Pantograph	
m_1: 6 kg; m_2: 7.12 kg; m_3: 5.8 kg; k_1: 9430 N/m; k_2: 14100 N/m; k_3: 0.01 N/m; c_1: 0 N·s/m; c_2: 350 N·s/m; F_{st}: 70 N; Interval: 200 m	

3.1 The Dynamic Performance of the Dual PCS in Curved Sections

Simulation cases are configured for curvature radii of 5500 m and 7000 m, with specific line parameters listed in Table 2. The corresponding maximum allowable train speeds are 220 km/h and 240 km/h, respectively.

Table 2. Parameters of curved section

Curvature Radius [m]	Superelevation [mm]	Speed [km/h]	a1 [mm]	a2 [mm]
5500	65	220	+300	-90
7000	70	240	+300	-150

3.2 Contact Force Evaluation Standards

The contact force of the PCS is a key indicator for assessing current collection quality, as it directly reflects the dynamic performance of the PCS. To ensure operational safety, strict standards have been established regarding the fluctuation range of contact force on actual operating lines. Common standards for this fluctuation range are listed in Table 3.

As indicated in Table 3, the standards require that the minimum contact force must exceed 0 N. This ensures that the pantograph head and contact wire maintain continuous contact during operation, safeguarding the quality of current collection and preventing arcing and electrical erosion, which could compromise operational safety.

Table 3. Specified contact force value in standards

Standard	Speed [km/h]	Mean Value [N]	Range [N]
EN 50119-2020 [19]	> 320	—	$0 < F \leq 400$
EN 50367-2012 [20]	> 200	$0.00047v^2 + 60 \leq F_m \leq 0.00097v^2 + 70$	—

3.3 Dynamic Performance Analysis in Curved Sections

A straight track condition is set as a control group for the curved track conditions. In this scenario, the pantograph operates at two speeds: 220 km/h and 240 km/h, corresponding to the maximum allowable train speeds for the R5500m and R7000m lines, respectively. The dynamic performance of the PCS at the maximum allowable speeds in curved sections is analyzed and compared with that on the straight track. Contact force results are presented in Table 4. It can be observed that:

(a) In both curved and straight sections, the contact force results indicate that the trailing pantograph is influenced by the vibration of the leading pantograph, resulting in a higher standard deviation of contact force;

(b) At the same speed, the contact force fluctuations for both pantographs are more pronounced in curved sections compared to straight sections;

(c) At the maximum allowable speed for curved sections, neither pantograph loses contact with the contact wire.

Table 4. Specified contact force value in standards

Speed	**220 km/h**				**220 km/h**			
Section type	R5500m		Straight		R7000m		Straight	
Pantograph	Leading	Trailing	Leading	Trailing	Leading	Trailing	Leading	Trailing
F_m [N]	116.9	118.0	115.7	116.5	125.5	126.3	125.1	125.5
σ(0-20Hz) [N]	16.5	19.2	13.5	15.9	17.9	20.9	14.6	18.6
$F_{\max}$ [N]	178.7	189.0	163.9	163.7	180.5	188.7	171.1	176.2
$F_{\min}$ [N]	63.9	42.3	73.3	67.5	77.64	58.2	79.4	64.2
Loss contact rate [%]	0	0	0	0	0	0	0	0

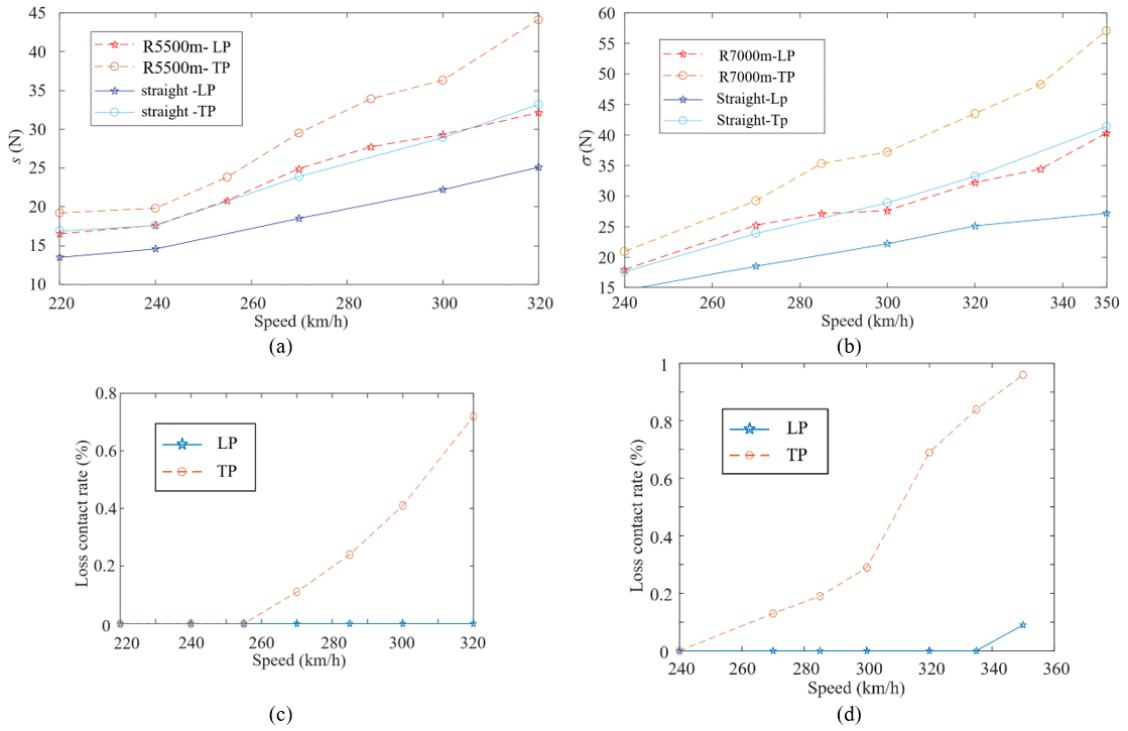

Figure 5. Dynamic results: (a) Standard deviation of contact force for the R5500 curved and straight section; (b) Standard deviation of contact force for the R7000 curved and straight section; (c) Loss contact rate of R5500 curved section; (d) Loss contact rate of R7000 curved section

3.4 Dynamic Performance in Curved Sections at Different Speeds

To examine the dynamic performance of the PCS in curved sections at higher speeds, six train speeds—220 km/h, 240 km/h, 270 km/h, 300 km/h, 320 km/h, and 350 km/h—are selected for simulating the dynamic performance of dual pantographs in both straight and curved sections. The results are displayed in Figure 5.

The results indicate that:

(a) As speed increases, the standard deviation of contact force for both pantographs in curved sections is consistently higher than in straight sections. Moreover, as speed increases, the PCS's dynamic performance in curved sections deteriorates more quickly, as indicated by a growing difference in the standard deviation;

(b) When the speed exceeds the maximum allowable limit for curved sections, the dynamic performance deteriorates significantly, leading to loss of contact;

(c) As speed increases, the trailing pantograph shows a higher rate of contact loss compared to the leading pantograph.

4 Optimization of Trailing Pantograph Dynamic Performance in Curved Sections

To maintain acceptable current collection quality at higher speeds in curved sections, the key issue lies in improving the dynamic performance of the trailing pantograph. This section proposes optimization methods from both the pantograph and catenary perspectives to address this problem.

4.1 Optimization Methods on the Pantograph Side

To mitigate excessive contact force fluctuations and prevent contact loss of the trailing pantograph at high speeds in curved sections, this paper proposes optimizing the pantograph-catenary dynamics by adjusting the static uplift force of the trailing pantograph.

Sixteen simulations were conducted for the R5500 curve section at operating speeds between 240 km/h and 320 km/h, and sixteen simulations for the R7000 curve section at speeds between 270 km/h and 350 km/h, with a speed interval of 5 km/h. For each speed and curve radius, nine cases were tested, increasing the static uplift force of the trailing pantograph by 50-95N in 5N increments. Based on the simulation results, the study evaluates whether adjusting the static uplift force in curved sections can enhance the dynamic performance of the trailing pantograph. The standard deviation of contact force and contact loss rate for the trailing pantograph from the simulations are shown in Figure 6.

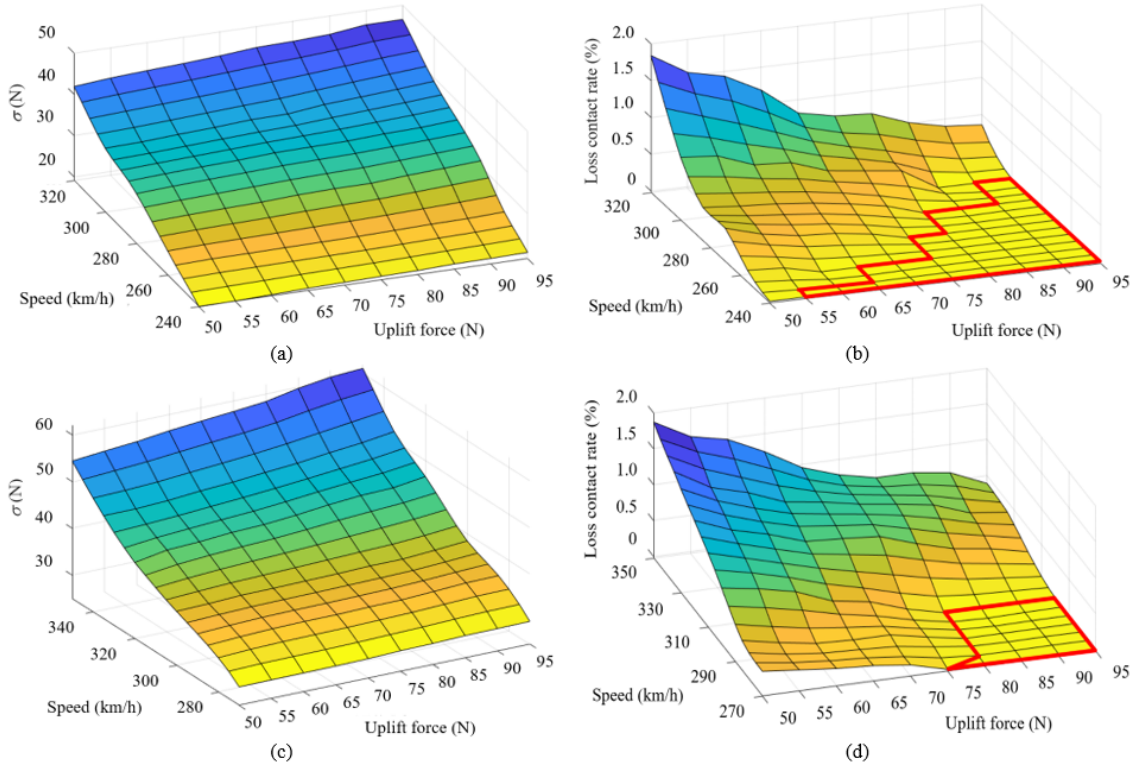

Figure 6. Dynamic results of trailing pantograph: (a) Standard deviation of contact force for the R5500 curved section; (b) Loss contact rate of R5500 curved section; (c) Standard deviation of contact force for the R7000 curved section; (d) Loss contact rate of R7000 curved section

It can be observed from Figure 6 that:

(a) The standard deviation for the trailing pantograph's contact force increases with the static uplifting force, and this effect intensifies as speed increases. At higher speeds, increasing the uplifting force results in a more significant rise in standard deviation;

(b) At a given speed, the loss contact rate of the trailing pantograph decreases with higher static uplifting force, with the reduction in contact loss being more evident at higher speeds;

(c) The red-framed areas in subgraphs (b) and (d) of Figure 6 highlight instances where the loss contact rate of the trailing pantograph is 0%. The critical speed at which the system achieves 0% contact loss in curved sections can reach up to 300 km/h, a significant improvement from the previous critical speeds of 255 km/h and 240 km/h. Increasing the static uplifting force markedly optimizes the dynamic performance of the trailing pantograph.

4.2 Optimization Methods on the Catenary Side

Increasing the contact wire tension and reducing the span length can significantly enhance the dynamic performance of the PCS. In this section, these two measures are evaluated for their impact on performance in curved sections.

4.2.1 Increase in contact wire tension

To assess the effect of increased contact wire tension on the contact force of PCS in curved sections, two tension increase combinations were applied, with the original tension serving as the control. The three conditions are presented in Table 5.

Table 5. Parameters of tension combinations

	Plan A	**Plan B**	**Plan C**
Contact wire tension (kN)	25	28.5	33
Messenger wire tension (kN)	20	20	20

Simulations at various speeds were performed on three tension combinations in the R5500m and R7000m curved sections, with the results presented in Figure 7 and Table 6.

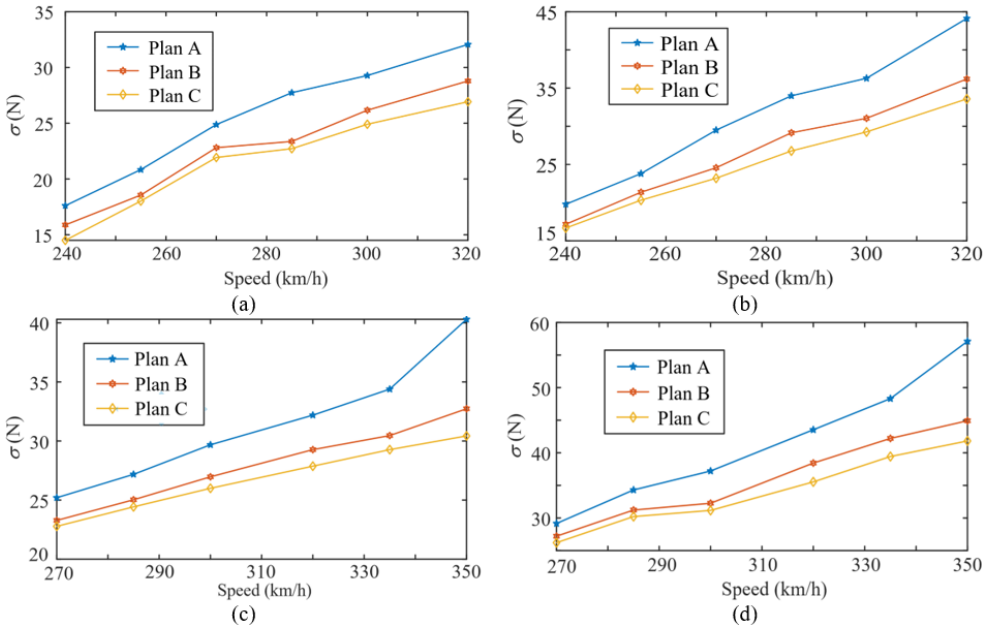

Figure 7. Standard deviation results: (a) Leading pantograph for the R5500 curved section; (b) Trailing pantograph for the R5500 curved section; (c) Leading pantograph for the R7000 curved section; (d) Trailing pantograph for the R5500 curved section

It can be observed that:

(a) Increasing the contact wire tension reduces the contact force's standard deviation for both pantographs in curved sections, and this effect intensifies as speed increases;

(b) Increasing the contact wire tension ensures that the trailing pantograph maintains contact at 300 km/h in both curved sections.

Table 6. Loss contact rate results

Speed (km/h)	Loss Contact Rate of R5500 (%)			Speed (km/h)	Loss Contact Rate of R7000 (%)		
	Plan A	Plan B	Plan C		Plan A	Plan B	Plan C
240	0	0	0	270	0.13	0	0
255	0	0	0	285	0.19	0	0
270	0.11	0	0	300	0.29	0	0
285	0.24	0	0	320	0.69	0.43	0.23
300	0.41	0.33	0	335	0.84	0.46	0.43
320	0.82	0.54	0.21	350	0.96	0.56	0.39

4.2.2 Reduce the span length

Table 7. Parameters of span length

	Plan A	Plan B	Plan C
Span length (m)	50	45	40

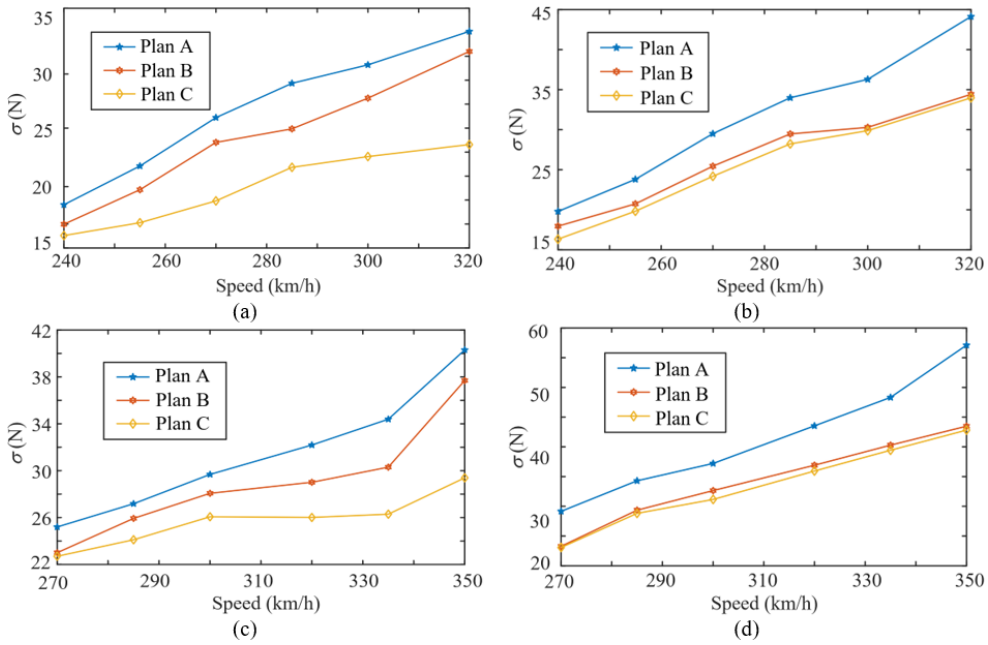

Figure 8. Standard deviation results: (a) Leading pantograph for the R5500 curved section; (b) Trailing pantograph for the R5500 curved section; (c) Leading pantograph for the R7000 curved section; (d) Trailing pantograph for the R5500 curved section

Table 8. Loss contact rate results

Speed (km/h)	Loss Contact Rate of R5500 (%)			Speed (km/h)	Loss Contact Rate of R7000 (%)		
	Plan A	Plan B	Plan C		Plan A	Plan B	Plan C
240	0	0	0	270	0.13	0	0
255	0	0	0	285	0.19	0	0
270	0.11	0	0	300	0.29	0	0
285	0.24	0	0	320	0.69	0.15	0.09
300	0.41	0	0	335	0.84	0.21	0.17
320	0.82	0.18	0	350	0.96	0.22	0.18

Two sets of span lengths were added to the catenary system, with the original span as a control. The three

conditions are shown in Table 7. Simulations at various speeds were conducted on these span lengths in the R5500m and R7000m curved sections, with the results displayed in Figure 8 and Table 8.

It can be observed that:

(a) Reducing the span improves the dynamic performance of the PCS in curved sections. When the span is shortened from 50 m to 45 m, the standard deviation of contact force for both pantographs decreases significantly. However, further reducing the span to 40 m results in no noticeable change in the trailing pantograph's contact force, while the leading pantograph continues to show improvement;

(b) Shortening the catenary span reduces the loss of contact rate of the trailing pantograph at high speeds in curved sections. This method is more effective than increasing the contact wire tension. It ensures no loss of contact at operating speeds of 300 km/h for the R5500 curve and 320 km/h for the R7000 curve.

5 Conclusions

This study has examined the dynamic behaviour of the PCS in curved sections, establishing a dynamic model to evaluate its performance and proposing optimisation strategies aimed at improving operational speeds. The findings suggest that significant speed enhancements in curved sections are feasible for high-speed railways. Although increasing speed tends to degrade the dynamic performance of the PCS and leads to a higher contact loss rate, these issues can be mitigated by optimising both pantograph and catenary components. The key conclusions of this research are as follows:

(a) At the same operating speed, the fluctuations in contact force are found to be more pronounced in curved sections than in straight sections, resulting in greater disparities in the dynamic performance of the trailing pantograph. Notably, when operating at the maximum allowable speed for curved sections, no contact loss is observed in either pantograph.

(b) As speed increases in curved sections, the standard deviation of the contact force for the trailing pantograph grows at a higher rate than that for the leading pantograph. This indicates a more significant deterioration in the dynamic performance of the trailing pantograph, which experiences contact loss earlier as speed increases.

(c) Several optimisation measures are identified to effectively mitigate contact loss and improve the allowable operating speed of the PCS in curved sections. These include increasing the static uplift force of the trailing pantograph, enhancing the tension of the contact wire, and reducing the span length of the catenary system.

These results provide important insights into the dynamic challenges faced by the PCS in curved sections and offer effective solutions to maintain operational performance at higher speeds. The proposed optimisation strategies are expected to contribute to the ongoing development of high-speed railway systems by improving their efficiency and reliability in complex track geometries.

Fundings

This paper was funded by National Natural Science Foundation of China (Grant No.: 52402452) and China Postdoctoral Science Foundation (Grant No.: 2024M752408).

Data Availability

The data used to support the findings of this study are available from the author upon request.

Conflicts of Interest

The author declares no conflicts of interest regarding this work.

References

[1] Y. Sun, D. Gao, Z. He, and H. Qiang, "Influence of electromagnet-rail coupling on vertical dynamics of EMS maglev trains," *Mechatron. Intell Transp. Syst*, vol. 1, no. 1, pp. 2–11, 2022. https://doi.org/10.56578/mits010102

[2] Z. Liu, Y. Song, Y. Han, H. Wang, J. Zhang, and Z. Han, "Advances of research on high-speed railway catenary," *J. Mod. Transport.*, vol. 26, pp. 1–23, 2018. https://doi.org/10.1007/s40534-017-0148-4

[3] Z. Liu, Y. Song, S. Gao, and H. Wang, "Review of perspectives on pantograph-catenary interaction research for high-speed railways operating at 400 km/h and above," *IEEE Trans. Transport. Electrific.*, vol. 10, no. 3, pp. 7236–7257, 2023. https://doi.org/10.1109/tte.2023.3346379

[4] Z. Xu, Z. Liu, and Y. Song, "Study on the dynamic performance of high-speed railway catenary system with small encumbrance," *IEEE Trans. Instrum. Meas.*, vol. 71, pp. 1–10, 2022. https://doi.org/10.1109/tim.2022.3191723

[5] Z. Xu, Y. Song, and Z. Liu, "Effective measures to improve current collection quality for double pantographs and catenary based on wave propagation analysis," *IEEE Trans. Vehicular Technol.*, vol. 69, no. 6, pp. 6299–6309, 2020. https://doi.org/10.1109/tvt.2020.2985382

[6] S. Bruni, J. Ambrosio, A. Carnicero *et al.*, "The results of the pantograph–catenary interaction benchmark," *Veh. Syst. Dyn.*, vol. 53, no. 3, pp. 412–435, 2015. https://doi.org/10.1080/00423114.2014.953183

[7] J. H. Lee, T. W. Park, H. K. Oh, and Y. G. Kim, "Analysis of dynamic interaction between catenary and pantograph with experimental verification and performance evaluation in new high-speed line," *Veh. Syst. Dyn.*, vol. 53, no. 8, pp. 1117–1134, 2015. https://doi.org/10.1080/00423114.2015.1025797

[8] Y. H. Cho, "Numerical simulation of the dynamic responses of railway overhead contact lines to a moving pantograph, considering a nonlinear dropper," *J. Sound Vib.*, vol. 315, no. 3, pp. 433–454, 2008. https://doi.org/10.1016/j.jsv.2008.02.024

[9] C. M. Pappalardo, M. D. Patel, B. Tinsley, and A. A. Shabana, "Contact force control in multibody pantograph/catenary systems," *Proc. Inst. Mech. Eng., Part K: J. Multi-body Dyn.*, vol. 230, no. 4, pp. 307–328, 2016. https://doi.org/10.1177/1464419315604756

[10] Y. Song, Z. Liu, F. Duan, Z. Xu, and X. Lu, "Wave propagation analysis in high-speed railway catenary system subjected to a moving pantograph," *Appl. Math. Model.*, vol. 59, pp. 20–38, 2018. https://doi.org/10.1016/j.apm.2018.01.001

[11] H. Wang, Z. Liu, A. Nunez, and R. Dollevoet, "Entropy-based local irregularity detection for high-speed railway catenaries with frequent inspections," *IEEE Trans. Instrum. Meas.*, vol. 68, no. 10, pp. 3536–3547, 2018. https://doi.org/10.1109/tim.2018.2881529

[12] W. Zhang, G. Mei, and J. Zeng, "A study of pantograph/catenary system dynamics with influence of presag and irregularity of contact wire," *Veh. Syst. Dyn.*, vol. 37, no. sup1, pp. 593–604, 2002. https://doi.org/10.1080/00423114.2002.11666265

[13] F. Duan, Y. Song, S. Gao, Y. Liu, W. Chu, X. Lu, and Z. Liu, "Study on aerodynamic instability and galloping response of rail overhead contact line based on wind tunnel tests," *IEEE Trans. Veh. Technol.*, vol. 72, no. 6, pp. 7211–7220, 2023. https://doi.org/10.1109/tvt.2023.3243024

[14] Y. Song, Z. Liu, H. Wang, X. Lu, and J. Zhang, "Nonlinear analysis of wind-induced vibration of high-speed railway catenary and its influence on pantograph–catenary interaction," *Veh. Syst. Dyn.*, vol. 54, no. 6, pp. 723–747, 2016. https://doi.org/10.1080/00423114.2016.1156134

[15] Y. Yao, D. Zou, N. Zhou, G. Mei, J. Wang, and W. Zhang, "A study on the mechanism of vehicle body vibration affecting the dynamic interaction in the pantograph–catenary system," *Veh. Syst. Dyn.*, vol. 59, no. 9, pp. 1335–1354, 2021. https://doi.org/10.1080/00423114.2020.1752922

[16] P. Antunes, J. Ambrósio, J. Pombo, and A. Facchinetti, "A new methodology to study the pantograph–catenary dynamics in curved railway tracks," *Veh. Syst. Dyn.*, vol. 58, no. 3, pp. 425–452, 2020. https://doi.org/10.1080/00423114.2019.1583348

[17] J. Xiong, Z. Xu, X. Lu, Z. Liu, and Y. Song, "Modeling and dynamic performance analysis of pantograph-catenary system in curved railway track," *J. China Railw. Soc.*, vol. 44, no. 8, pp. 25–35, 2022. https://doi.org/10.3969/j.issn.1001-8360.2022.08.003

[18] Z. Xu, Y. Song, and Z. Liu, "Stress analysis and fatigue life prediction of contact wire located at steady arms in high-speed railway catenary system," *IEEE Trans. Instrum. Meas.*, vol. 71, pp. 1–12, 2022. https://doi.org/10.1109/tim.2022.3144747

[19] British Standards Institution, "BS EN 50119: Railway applications. fixed installations. electric traction overhead contact lines," British Standards Online (BSOL), 2020. https://landingpage.bsigroup.com/LandingPage/Undated?UPI=000000000019984474

[20] British Standards Institution, "BS EN 50367: Railway applications. fixed installations and rolling stock. criteria to achieve technical compatibility between pantographs and overhead contact line," British Standards Online (BSOL), 2020. https://landingpage.bsigroup.com/LandingPage/Undated?UPI=000000000030228825